Urban Studies and Public Administration
Vol. 6, No. 3, 2023
www.scholink.org/ojs/index.php/uspa
ISSN 2576-1986 (Print) ISSN 2576-1994 (Online)

Original Paper

Mechanical Characteristics of Precast Cracked Concrete under Freeze-Thaw-Load Action

Bin Zhao[1], Shiwei Shen[1], & Poning Zhang[1]

[1] College of Civil Engineering, Jilin University, Changchun, China

Received: July 21, 2023 Accepted: August 19, 2023 Online Published: September 6, 2023

doi:10.22158/uspa.v6n3p45 URL: http://dx.doi.org/10.22158/uspa.v6n3p45

Abstract

Four types of precast double-cracked concrete specimens and non-cracked control group were prepared, and the specimens were subjected to freezing and thawing cycles and uniaxial compression tests, with a total of five freezing and thawing cycles, namely 0, 25, 50, 75 and 100, in order to analyse the fracture phenomena and mechanical properties of the specimens after freezing and thawing in uniaxial compression, and to determine the damage variables of the precast cracked concrete under the action of freezing and thawing loads on the basis of strain energy and fracture mechanics theories. The test results show that: (1) the crack aggregation mode generated by the compression damage of precast cracked specimens is mainly influenced by the crack inclination angle, when the crack inclination angle is 30°, the specimen undergoes wing tension aggregation, and when the crack inclination angle is 60°/90°, the specimen undergoes a mixed tension-shear aggregation mode; (2) After the freeze-thaw cycle test, the degree of deterioration of the prefabricated cracked specimens is significantly higher than that of the non-cracked specimens, and the loss of compressive strength and Young's modulus of the specimens with crack inclination angle of 60° and 90° is the most severe, and the decrease of the stress-strain curve is the most obvious; (3) Based on fracture mechanics and damage-strain energy to derive the damage variables of the prefabricated cracked loaded specimens, and based on the Weibull function and the principle of equivalent effect of Lemaitre effect, the damage variables under freeze-thaw loading are also derived based on the Weibull function and Lemaitre equivalent strain principle.

Keywords

prefabricated double cracks, freeze-thaw cycles, damage variables

1. Introduction

In the actual project, most of the concrete with initial cracks, and then subjected to freeze-thaw cycles lead to different degrees of damage in the use of the process, which leads to a decline in the strength of concrete affecting the safe use of structures. Some scholars have studied the effect of precast cracks on the frost resistance of concrete, Wardeh G et al. (2015) conducted freeze-thaw and three-point bending tests on pre-slotted concrete beams, and found that freezing and thawing would lead to a decrease in their mechanical properties, an increase in fracture energy, and the tensile strength showed a more obvious degree of deterioration of cracks after freezing and thawing. Cheng et al. (2016) produced cracks with different widths in the specimens by loading, and performed the Freeze-thaw cycle tests, found that cracks increased the specimen spalling quality and decreased the compressive strength, and the cracks corroded the reinforcement inside the specimen the most severely. Yu Jianfu (2015) improved the method of making precast cracks and investigated the trend of mass loss rate and relative dynamic modulus of elasticity of cracked concrete under freeze-thaw action, and the results showed that the precast cracks significantly aggravated the degree of time damage and weakened the durability of its frost resistance. Yu Xiaomin et al. (2010) investigated the fracture properties of precast cracked concrete under freeze-thaw cycling conditions, and the results showed that the fracture energy of precast cracked specimens decreases in a quadratic term relationship with the increase in the number of freeze-thaw cycles. Chen Youliang et al. (2011, 2019) investigated the mechanical and fracture properties of concrete specimens containing macro cracks after freeze-thaw cycling, and found that macro cracks accelerated the deterioration of specimens by freezing and thawing, but the relative depths of the initial cracks had basically no effect on the fracture toughness.

Scholars at home and abroad have also carried out extensive research on concrete damage models, with less research on the damage variables of crack-containing concrete, and the damage variables of concrete under freeze-thaw loading state are mainly defined by elastic modulus, among which the Lemaitre's assumption and Weibull's function are more widely used for the representation of the damage variables under freeze-thaw loading (Li et al., 2020; Sun, Xin, & Zou, 2019; Wang et al., 2020; Xiao, 2013; Yi et al., 2013; Yu, Ma, & Yan, 2017; Chen et al., 2019; Chen et al., 2018; Li, Qiao, & Zhu, 2020; Wang, B., Wang, F., & Wang, Q., 2018; Xiao & Niu, 2009). In related research progress, Ditao Niu et al. (Niu & Xiao, 2010) chose a three-parameter Weibull function to establish the probability curve of damage versus the number of cycles under freeze-thaw concrete and regressed it to obtain a cumulative damage model. Wang Boxin et al. (2019) established a macro-micro damage model based on Lemaitre's assumption and carried out experimental validation to derive the expression of the damage variables for a four-parameter cubic function. Qiu et al. (2020) established a freeze-thaw damage model for CGC using the relative kinetic-elastic modulus, and at the same time established a load damage model based on the acoustic emission from the CGC during the compressive damage process. The research on the freeze-thaw damage characteristics of precast cracked concrete is still insufficient and lacks the research on the mechanical property law after freeze-thaw and the derivation and calculation of damage variables, so the mechanical properties and damage variables of precast cracked concrete need to be further studied. In this paper, four types of precast cracked concrete specimens were subjected to freeze-thaw cycle and uniaxial compressive strength tests, and controlled with the non-cracked specimens, and the number of freeze-thaw cycles was designed to be 0, 25, 50, 75, and 100, respectively, so as to analyse the compressive damage of each group of specimens after freezing and thawing and investigate the relationship of compressive strength, stress-strain curve, and elasticity modulus with the precast cracks and the number of freeze-thaw cycles, and establish the relationship between freeze-thaw cycles and compressive strength and the number of freeze-thaw cycles. The relationship between compressive strength, stress-strain curve and modulus of elasticity with precast cracks and the number of freeze-thaw cycles is investigated to establish the damage variables of precast cracked concrete under freeze-thaw-load coupling.

2. Overview of the Experiment

2.1 Specimen Preparation

The size of 150mm×150mm×150mm concrete cube specimen is selected for this test, and C30 concrete is selected for the test according to the "Specification for the Design of Proportioning of Ordinary Concrete" (JGJ-55-2011) and combined with the engineering experience. The specimen mix ratio is shown in Table 1, in which the cement is ordinary silicate cement with strength class 32.5, coarse aggregate is gravel with particle size less than 20mm, fine aggregate is river sand and tap water.

Table 1. Concrete Specimen Material Mix Ratio

materials	water	cement	sand	crushed stone
proportions	0.38	1	1.11	2.72

Selected 1mm thick steel sheet for crack prefabrication, specimen moulding inserted and control crack length of 25mm, steel sheet through the specimen to be withdrawn after the initial setting of the concrete, the test was designed a total of four types of parallel cracks A, B, C, D, in order to explore the overlap defects under the different crack inclination angle of the impact of the concrete damage form. The specific parameters and schematic diagrams of the prefabricated cracks are shown in Table 2, respectively, where α is the crack inclination angle (30°, 60° and 90°) and β angle is the rock bridge angle (90°, 120°), fifteen concrete specimens are prepared for each type of cracks and fifteen concrete specimens without cracks are prepared as Group E for the comparison test.

Table 2. Specimen Design Parameters

Crack form	α	β
A	30°	120°
B	60°	90°
C	60°	120°
D	90°	120°
E	uncracked	

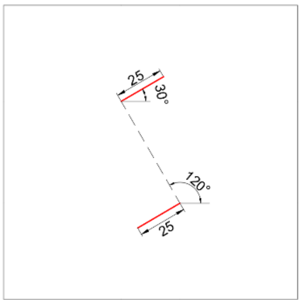

(A)

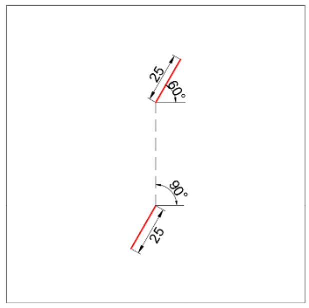

(B)

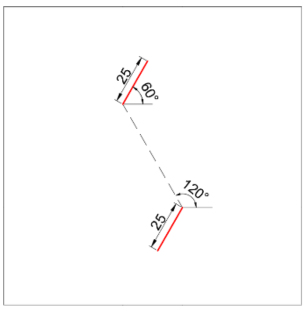

(C)

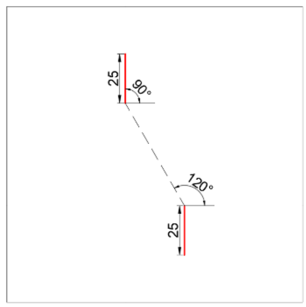

(D)

2.2 Freeze-thaw Cycle Test

The test refers to the "Standard of Test Methods for Long-term Performance and Durability of Ordinary Concrete" (GB/T 50082-2009), which selects the slow-freezing method for the freeze-thaw cycle and formulates the freezing time and thawing time of each cycle as 6 hours. The number of freezing and thawing cycles designed for the test was 0, 25, 50, 75 and 100 times, and each crack type was divided into five groups according to the number of freezing and thawing cycles, and three specimens were numbered in each group. The specimen number is defined according to the crack type, the number of freeze-thaw cycles and the order in the group, e.g., A-25-2 means A type crack, 25 freeze-thaw cycles, the second specimen in the group.

3. Experimental Phenomena

Prefabricated cracked specimens will produce new cracks in the process of compression, mainly wing cracks, anti-wing cracks and secondary cracks (as shown in Figure 1), and the production of new cracks reflects the randomness and uncertainty of the distribution of materials and defects inside the specimen. At the same time, with the increase in the number of freeze-thaw cycles, the internal defects of the specimen will also develop and produce cracks, and when the internal and external cracks continue to develop and interact with each other, the specimen will produce a more complex crack aggregation pattern.

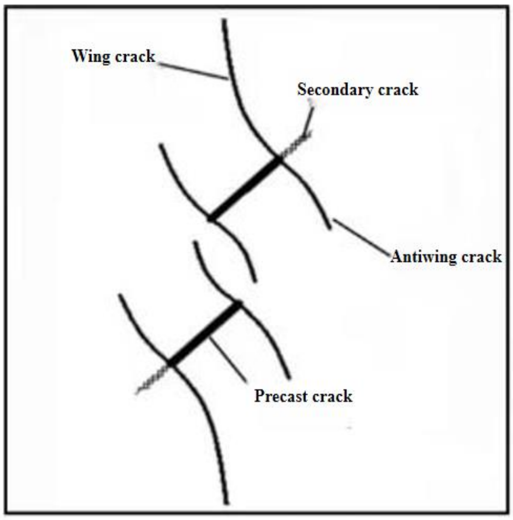

Figure 1. Schematic Diagram of Derived Cracks

The four different forms of cracks produce different degrees of agglomeration patterns during compression damage, as seen in Figure 2(1), the A-type crack under pressure without freeze-thaw occurs through damage along a single crack, and there is no obvious correlation between the two prefabricated cracks; after the action of the freeze-thaw cycle, the damage form of the A specimen manifests itself as a multi-flanking crack produced by the end of the two prefabricated cracks with the anti-flanking cracks penetrating through the damage of each other, as shown in Figure 2(2).

(1) (2)

Figure 2. Schematic Diagram of Crack Penetration Pattern of Type A

Type B specimen without freeze-thaw cycle under pressure damage crack agglomeration pattern is the same as type A (as shown in Figure 3(1)), after experiencing freeze-thaw cycle the top of the upper prefabricated crack produces secondary cracks, and the bottom produces anti-wing cracks and the lower prefabricated cracks of the wing cracks intersected and damaged, as shown in Figure 3(2).

(1) (2)

Figure 3. Schematic Diagram of Crack Penetration Pattern of Type B

Type C cracked specimens without freezing and thawing were also damaged along the lower prefabricated cracks through and through, and the two prefabricated cracks were not more related, as shown in Figure 4(1). After the freeze-thaw cycle, Figure 4(2) shows that the damage pattern is similar to that of type A. The wing cracks generated by the two prefabricated cracks are connected with the counter-wing cracks, and the crack expansion path is more zigzag and produces a lot of microcracks.

(1) (2)

Figure 4. Schematic Diagram of C-crack Penetration Pattern

The D-type crack in Figure 5(1) produces a distinct wing crack in the upper crack without freeze-thaw cycles, and the two prefabricated cracks intersect through secondary cracks. After an increasing number of freeze-thaw cycles, the wing cracks sprouting from the inner ends of the two cracks connect with the counter-wing cracks and penetrate through the original prefabricated cracks, as shown in Figure 5(2).

(1) (2)

Figure 5. Schematic Diagram of Crack Penetration Pattern in Group D

The four kinds of cracked specimens without freeze-thaw cycle new crack generation and expansion mode is basically the same, are from the lower prefabricated crack inner end and outer end of the first wing crack (group D is more obvious), the upper prefabricated crack basically does not appear damage, but before the wing crack further spread, the secondary crack rapid development and extend to the edge of the specimen, this shear agglomeration mode is due to the prefabricated cracks through the specimen resulting in high pressure when compression shear stress concentration phenomenon. With the action of freeze-thaw cycle, the prefabricated crack end of each group of specimens produces obvious wing cracks, and the aggregation mode of the specimen with type A crack (α=30°) is the wing tension mode, and the three types of specimens, B, C, and D, are the mixed tension-shear mode. It can be seen that when the crack inclination angle is 30°, the prefabricated crack mainly produces wing cracks and anti-wing cracks occurring tension damage, at this time the specimen is mainly subjected to tensile stress damage; when the crack inclination angle of 60°/90°, the specimen receives the superposition of the tensile and shear stresses, which leads to the occurrence of the specimen of the tensile-shear mixed damage.

4. Test Results

4.1 Stress-strain Curve

According to the stress-strain data of each group of concrete specimens obtained from the uniaxial compressive strength test of concrete, the stress-strain curves of each group of specimens under different numbers of freezing and thawing cycles were plotted, as shown in Figure 6.

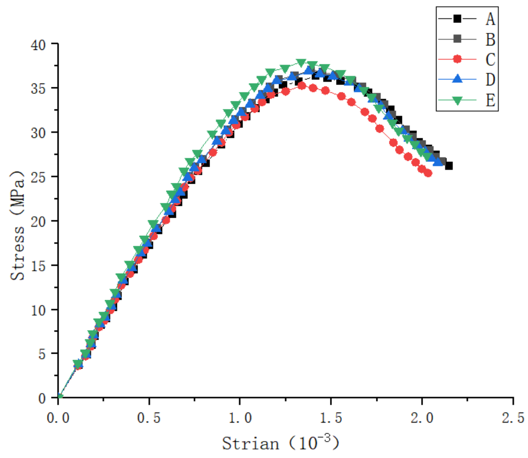

(1) 0 freeze-thaw cycles

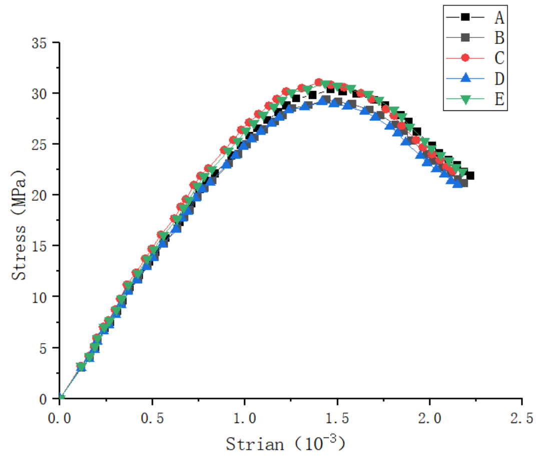

(2) 25 freeze-thaw cycles

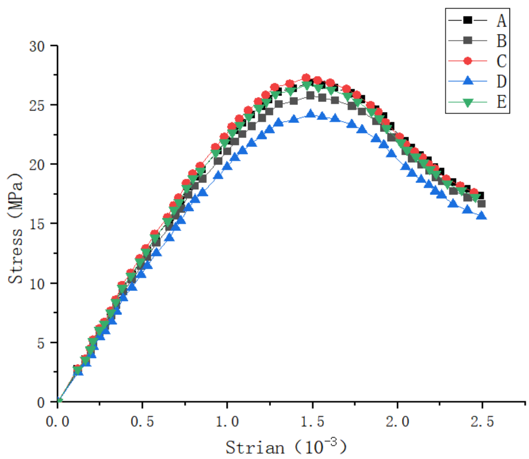

(3) 50 freeze-thaw cycles

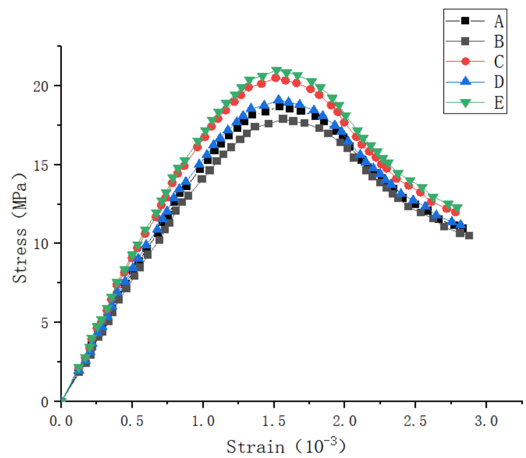

(4) 75 freeze-thaw cycles

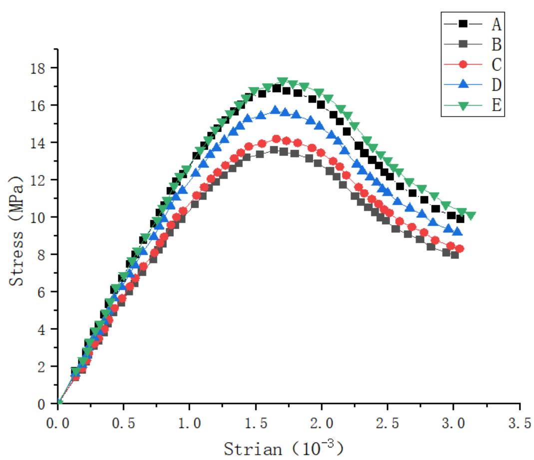

(5) 100 freeze-thaw cycles

Figure 6. Stress-strain Curves of Each Group of Specimens under Different Numbers of Freeze-thaw Cycles

As can be seen from the stress vertical axis in the figure, the peak strength of each group of specimens decreases continuously with the increase of the number of freeze-thaw cycles. The rising stage of the stress-strain curves of each group can be divided into three stages: (1) the first stage is when the axial load is initially applied, and the specimens of each group are in the elastic working state, and the deformation of the specimens at this stage is mainly the elastic deformation of the internal aggregate and the compression density of the primary pores; (2) the second stage is the stage of the steady development of the cracks, and at this time, the stress-Strain curve gradually turned to nonlinear, the specimen internal microcracks and prefabricated cracks continue to develop, and the compressive strength gradually reached the critical point; (3) the third stage is the stage of plastic deformation, the specimen's cracks rapidly expand and penetrate into each other, and the concrete stress also reached the peak point.

When the specimens did not experience freeze-thaw cycles, the stress-strain curves of each group of specimens were close to each other, and the peak stress and peak strain of each group of specimens did not differ much. When the number of freeze-thaw cycles reaches 25 to 75 times, the peak stress difference of each group of specimens is gradually obvious and the slope of the elastic phase gradually becomes smaller, and the slope of the elastic phase gradually becomes smaller, indicating that with the increase of the number of freeze-thaw cycles, the degree of damage to the concrete increases, and the stiffness decreases, and the most obvious decrease in the stress-strain curve is the specimen of group B, which can be seen that the effect of freeze-thaw cycles on the B cracks is the most. Maximum. After 100 freeze-thaw cycles, it is obvious that the decrease in peak strength of precast cracked specimens is greater than that of non-cracked concrete specimens, and the stress-strain curves of the specimens with precast cracks have a more gentle trend than that of non-cracked specimens, in which the curve of group B specimens is the most gentle, followed by group C. The crack inclination of both groups B and C is 60°. Compared with groups A and D, it can be seen that when $\alpha=60°$ 、$\beta=90°$, the internal damage of the specimen after freezing and thawing is more serious, resulting in more damage after compression.

4.2 Changes in Modulus of Elasticity

The modulus of elasticity of concrete is an important index to measure the performance of concrete, and it can also respond to the relationship between stress-strain of concrete, so as to show the structural deformation and internal damage of concrete more intuitively. In this paper, based on "Code for the Design of Concrete Structures" (gb 50010-2010, 2015), the slope of the line connecting the origin of the stress-strain curve and the point where the stress is 50% compressive strength is selected as the elastic modulus parameter of the specimen, and the specific values are shown in Table 3, and according to the table data, the elastic modulus is plotted with the change of crack inclination angle and the rock bridge angle as the image shown in Figure 7.

Table 3. Modulus of Elasticity of Concrete for Different Cases

Number of freeze-thaw cycles	Modulus of elasticity (GPa)				
	Group A	Group B	Group C	Group D	Group E
0	30.2	30.5	29.7	30.4	30.8
25	27.6	27.1	27.9	27.0	27.8
50	25.9	25.4	26.1	24.6	25.8
75	21.6	21.2	22.6	21.9	22.9
100	19.6	18.4	18.8	19.8	20.8

According to the test results in Table 3, it can be seen that the elastic modulus values of each group of concrete specimens did not differ significantly when they were not subjected to freeze-thaw cycles, indicating that there was no significant difference in the effect of the precast cracking styles on the elastic modulus when they were not subjected to freeze-thaw action. With the continuous action of freeze-thaw cycles, the modulus of elasticity of each group of specimens decreased, indicating that microcracks inside the specimens were derived and developed, resulting in loose concrete structure and reduced stiffness. Compared with the intact specimens, the loss of modulus of elasticity of the precast cracked specimens after the freeze-thaw cycle was more obvious because the internal cracks generated by freeze-thaw continued to develop and intersected with the precast cracks, which led to more intense internal damage and the specimen’s ability to produce elastic deformation became increasingly poor.

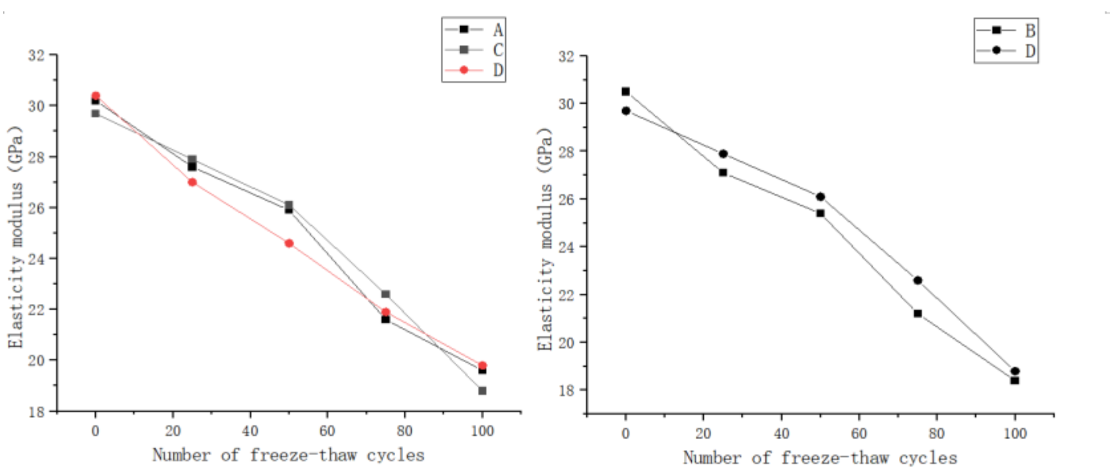

Figure 7. Graphical Representation of the Variation of Elastic Modulus of the Specimen with the Rock Bridge Angle

As seen in Figure 7, the elastic modulus shows a good linear relationship with the number of freeze-thaw cycles and decreases with the increase in the number of cycles. When the rock bridge angle β=120°, the elastic modulus of α=90° decreased to a greater extent at 0-75 cycles, and the elastic modulus of α=60° specimen decreased abruptly at 75-100 cycles, and it is presumed that the internal cracks at α=90° developed too fast at lower cycle times, while the internal cracks of α=60° specimen at 75 cycles before deriving to intersect with the prefabricated crack. When the crack inclination angle α=60°, the modulus of elasticity of β=90° specimens without cycling was higher than that of β=120°, but with the freeze-thaw cycling action the internal cracks gradually intersected with the prefabricated cracks, and the modulus of elasticity of the specimens in each group of B-type cracks decreased faster, which indicated that the freeze-thaw cycling caused a more serious degradation of B-type cracks than C-type cracks. In conclusion, the freeze-thaw cycle has the greatest influence on B-type cracks (α=60°, β=90°), and when the number of cycles reaches 100 times, the deterioration of B-type cracks is the most obvious, and the damage of internal structure is the most serious.

5. Damage Variables in prefabricated Cracked Specimens under Freeze-thaw-load Coupling

5.1 Damage Variables for Prefabricated Cracks Subjected to Loads

Four types of prefabricated cracked specimens uniaxial compression in two cracks composite damage state, fracture conditions are more complex, so based on the fracture mechanics and damage strain can be based on the calculation formula of the damage variables, combined with the solution of the strength factor of the fractured rock body method to derive the damage variables suitable for this test.

When a single crack exists in the specimen, the state of stress on the cracked surface during uniaxial compression is (Cao, 2021):

$$\begin{cases} \sigma_x = \sigma \sin^2\beta \\ \tau = \dfrac{1}{2}\sigma \sin 2\beta \\ \sigma_y = \sigma \cos^2\beta \end{cases} \tag{1}$$

Since the design of this test prefabricated crack width of 1mm and with the width of the freeze-thaw slightly increased, so there is no interaction force between the crack surface, due to uniaxial loading crack surface is only subject to stress σ_1 , the effective positive stress and shear stress of the crack surface is:

$$\begin{cases} \sigma_1 = \sigma_1 \cos^2\alpha \\ \tau_1 = \dfrac{\sin 2\alpha}{2}\sigma_1 \end{cases} \tag{2}$$

Thus the effective stress factor for single crack is:

$$\begin{cases} K_{I0} = \sigma_1 \cos^2\alpha \sqrt{\Pi a} \\ K_{II0} = \dfrac{1}{2}\sigma_1 \sin 2\alpha \sqrt{\Pi a} \end{cases} \tag{3}$$

Where: K_{I0}、K_{II0} is the stress intensity factor for type I and II fissures, respectively; a is the half-length of the fissure and ω is the width of the specimen.

Since the prefabricated cracks belong to a single set of two rows of cracks (Liu & Su, 2016), the effective stress intensity factor is given by Eq. (3):

$$K_I = f(a, b, d) K_{I0};\ K_{II} = f(a, b, d) K_{II0} \tag{4}$$

Where: f (a, b, d) is the crack influence coefficient, take 1.505 (Liu & Su, 2016).

According to the damage strain energy theory, elastomer due to the presence of cracks leads to an increase in additional strain energy U_1 for:

$$U_1 = \int_0^A G dA = \frac{1-\nu^2}{E}\int_0^A (K_I^2 + K_{II}^2) dA \tag{5}$$

Where: G is the strain energy release rate; ν is the Poisson's ratio of the rock mass; A is the surface area of the fissure. For double cleavage, A=2Ba, B is the cleavage width, and a is the joint half-length.

Assume that the volume of the study object is V and the elastic strain energy change of the elastomer due to the presence of the joints is:

$$\Delta U^E = V\left[\frac{\sigma^2}{2E(1-D)^2} - \frac{\sigma^2}{2E}\right] \tag{6}$$

Both U_1 in Eq. (5) and ΔU^E in Eq. (6) are the amount of change in elastic strain energy due to cleavage, therefore they are equal, i.e.

$$\frac{1-\nu^2}{E}\int_0^A (K_I^2 + K_{II}^2) dA = V\left[\frac{\sigma^2}{2E(1-D)^2} - \frac{\sigma^2}{2E}\right] \tag{7}$$

From Eq. (4) and Eq. (7), the damage variables of precast cracked concrete specimens under uniaxial compression are:

$$D_{pc} = 1 - \left\{1\Big/\left[1 + \frac{37.72Ba^2}{V} f^2(a,b,d)\cos^2\alpha\ (\sin\alpha - \cos\alpha\tan\varphi)^2\right]\right\}^{-1} \tag{8}$$

Where: D_{pc} is the damage variable for precast cracks; φ is the angle of rupture of the concrete specimen, taken as 45°.

5.2 Freeze-thaw-loading Damage Variables

Based on the theory of concrete damage mechanics (Li, 2017), the modulus of elasticity after freeze-thaw cycle is selected as the damage variable, which is defined as:

$$D_{fc} = 1 - \frac{E_{\mathrm{fc}}}{E_0} \tag{9}$$

where: $\mathrm{D_{fc}}$ -Freeze-thaw damage variable; $\mathrm{E_{fc}}$ -Modulus of elasticity of concrete after freeze-thaw damage; $\mathrm{E_0}$ -Modulus of elasticity of concrete without freeze-thaw.

Under uniaxial compression, the number of damaged micromonomers in concrete is defined as $\mathrm{N_d}$, the total number of $\mathrm{N_t}$, then the interrelationship can be expressed as:

$$N_d = N_t \int_0^{\varepsilon} P(F)dF = N_t\left[1 - e^{-\left(\frac{\varepsilon}{a}\right)^b}\right] \tag{10}$$

Based on the Weibull function, the damage probability density distribution function for concrete is derived as:

$$P(F) = \frac{a}{b}\left(\frac{F}{b}\right)^{a-1} \cdot e^{-\left(\frac{F}{b}\right)^a} \tag{11}$$

Where: f is the concrete micro-element strength distribution variable; a, b are Weibull distribution parameters.

Thus the damage variable of concrete under load can be expressed as D_{uc} :

$$D_{uc} = \frac{N_d}{N_t} = 1 - e^{-\left(\frac{\varepsilon}{a}\right)^b} \tag{12}$$

According to the Lemaitre equivalent strain principle (Lemaitre, 1985), the first stage damage is the concrete freeze-thaw damage, the second stage damage is the freeze-thaw-load coupling effect, and the damage ontological relationship of the two stages are respectively:

$$\begin{cases} \sigma_{\mathrm{fc}} = \mathrm{E_0}\varepsilon(1 - \mathrm{D_{fc}}) \\ \sigma = \mathrm{E_{fc}}(1 - \mathrm{D_{uc}}) \end{cases} \tag{13}$$

Where: σ_{fc} -Stress after freezing and thawing; D_{uc} -Damage variable resulting from loading action.

The damage factor under freeze-thaw-load coupling can be obtained by bringing Eqs. (9) and (12) into Eq. (13):

$$D_m = 1 - \frac{E_{\mathrm{fc}}}{E_0} \cdot e^{-\left(\frac{\varepsilon}{a}\right)^b} \tag{14}$$

Where: $\mathrm{D_m}$ represents the total damage variable for concrete that freezes and thaws and is subjected to loading.

The values of a and b in the damage variables under freeze-thaw-load coupling are only relevant to the freeze-thaw loading effect, and calculations using the peak point method have:

$$\frac{d\sigma}{d\varepsilon}_{\varepsilon=\varepsilon_p} = E_{fc} \cdot e^{-\left(\frac{\varepsilon p}{a}\right)^b} + E_{fc} \cdot \varepsilon_p \cdot e^{-\left(\frac{\varepsilon p}{a}\right)^b} \cdot (-b) \cdot \left(\frac{\varepsilon_p}{a}\right)^{b-1} = 0 \tag{15}$$

$$\sigma_p = E_{fc} \cdot \varepsilon_p \cdot e^{-\left(\frac{\varepsilon p}{a}\right)^b} \tag{16}$$

Combining Eq. (15) and Eq. (16) yields:

$$\begin{cases} a = \sqrt[b]{b} \cdot \varepsilon_p \\ b = \dfrac{1}{\ln \dfrac{E_{fc}\varepsilon_p}{\sigma_p}} \end{cases} \tag{17}$$

in the formula: σ_p and ε_p are the peak stress and peak strain of concrete for different cases, respectively.

5.3 Damage Variables of Prefabricated Cracked Specimens Subjected to Freeze-thaw-loading

The damage coupling at different scales is manifested as the coupling of damage variables, and in this test, under the action of freeze-thaw cycles, the fissure damage variables of macroscopic cracks are considered at the same time, so the basic assumption of damage mechanics-Lemaitre's assumption should be followed, as shown in Figure 8. Figure 8 (a)-(d) are represented as specimens containing macroscopic cracks and freeze-thaw damage, specimens containing only macroscopic cracks, specimens subjected to freeze-thaw damage only, and hypothetical completely undamaged specimens with elastic modulus E_t, E_{pc}, E_m, E_0, respectively, and at the same time ε_t 、ε_{pc}、ε_m、ε_0 are the corresponding strains, respectively. Based on the damage coupling condition, it can be known:

$$\varepsilon_t = \varepsilon_{pc} + \varepsilon_m - \varepsilon_0 \tag{18}$$

Based on the generalised Hooke's law, the stress-strain transformation equation can be obtained at the elastic deformation stage:

$$\frac{\sigma}{E_t} = \frac{\sigma}{E_{pc}} + \frac{\sigma}{E_m} - \frac{\sigma}{E_0} \tag{19}$$

Taking the modulus of elasticity to represent the deterioration within the specimen, the following equation can be derived:

$$\begin{cases} E_t = E_0(1 - D_t) \\ E_{pc} = E_0(1 - D_{pc}) \\ E_m = E_0(1 - D_m) \end{cases} \tag{20}$$

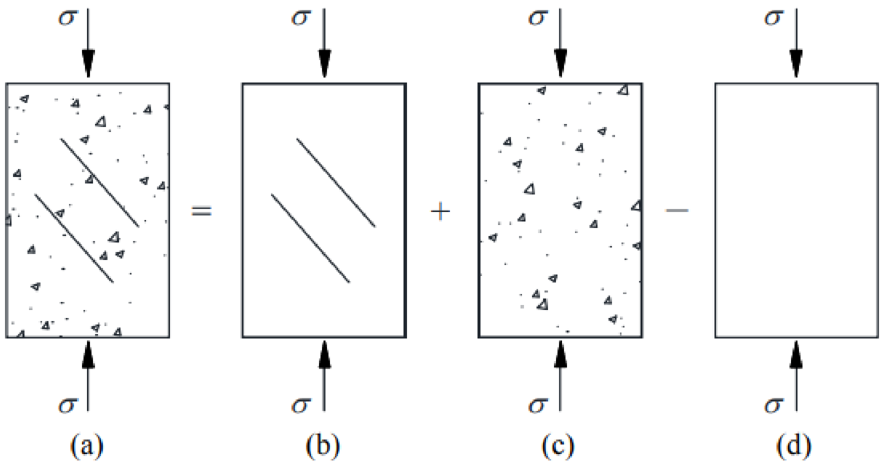

Figure 8. Strain Equivalent Schematic

Substituting Eq. (20) into Eq. (19) and collating and simplifying gives the damage variable for precast cracked concrete under freeze-thaw-load coupling as:

$$D_{\mathrm{t}} = 1 - \frac{(1 - D_{pc})(1 - D_m)}{1 - D_{pc} D_m} \tag{21}$$

6. Conclusion

In this paper, four types of precast cracked and uncracked concrete specimens were subjected to freeze-thaw cycles and uniaxial compression experiments, and the damage, compressive strength, stress-strain curves and modulus of elasticity of the tested specimens were analysed, and the following conclusions were obtained based on the mechanics of fracture and the damage-strain energy to derive the damage variables:

(1) The damage of prefabricated cracked specimens after freeze-thaw cycles is more serious than that of non-cracked specimens, the prefabricated cracked specimens without freeze-thaw are subjected to high shear stress concentration phenomenon due to the prefabricated crack running through the specimens, which leads to the formation of shear agglomeration mode of the cracks; the prefabricated cracked specimens after freeze-thaw cycles produce more cracks obviously, and the specimen cracks are in the tension-agglomeration mode of the flanks when the inclination angle of the cracks is 30° and the cracks are in the mixed tension-shear damage mode of the specimens when the inclination angle of the cracks is 60°/90°. When the crack inclination angle is 60°/90°, the specimen cracks in a mixed tension-shear damage mode.

(2) After the four types of precast cracked specimens underwent freeze-thaw cycle test, the deterioration degree was obviously higher than that of non-cracked specimens, and the loss of compressive strength and modulus of elasticity was most serious in B-type cracks (α=60°, β=90°), and the decrease of stress-

strain curve was most obvious, and the analysis showed that when the crack inclination angle of 60° was similar to that of the through rupture angle of the concrete under compression damage and β= 90° the precast cracks were overlapping cracks, resulting in the most serious deterioration of the specimens. 90° when the prefabricated cracks are overlapping cracks, the joint effect of internal cracks and prefabricated cracks is more intense, resulting in the most serious specimen deterioration.

(3) Based on fracture mechanics and damage strain energy, the compressive damage variables of prefabricated cracks in a double-crack compliant state are derived and calculated, and the damage variables under freeze-thaw loading are also derived based on the Weibull function and Lemaitre's principle of equivalent strain.

Reference

Cao, C. (2021). *Research on the strength characteristics test and damage variable calculation method of rock body with multiple parallel fissures type*[D]. Three Gorges University.

Chen, S., Ren, J., Song, Y. et al. (2019). Salt Freeze-Thaw Damage Characteristics of Concrete based on Computed Tomography. *Tehnicki Vjesnik-Technical Gazette*, *26*(6), 1753-1763. https://doi.org/10.17559/TV-20190819080524

Chen, X., Chen, C., Liu, Z. et al. (2018). Compressive behaviour of concrete under high strain rates after freeze-thaw cycles. *Computers and Concrete*, *21*(2), 209-217.

Chen, Y. L., Liu, M. L., & Jiang, L. H. (2011). Experimental study on mechanical properties of concrete containing macro cracks by freezing and thawing. *Journal of Civil Engineering*, *44*(S2), 230-233.

Cheng, Y., Zhang, Y., Jiao Y., et al. (2016). Quantitative analysis of concrete property under effects of crack, freeze-thaw and carbonation. *Construction and Building Materials*, *129*, 106-115. https://doi.org/10.1016/j.conbuildmat.2016.10.113

gb 50010-2010. (2015). *Code for the design of concrete structures* [S].

GB/T 50082-2009. *Standard for long-term performance and durability test methods for ordinary concrete* [S]. Beijing: China Construction Industry Press.

Hang, M., Cui, L., Wu, J. et al. (2020). Freezing-thawing damage characteristics and calculation models of aerated concrete. *Journal of Building Engineering*, *28*. https://doi.org/10.1016/j.jobe.2019.101072

JGJ-55-2011. *Specification for the design of mix ratio of ordinary concrete* [S]. Industry Standard-Construction Industry (CN-JG), 2011.04.22.

Jin, S., Zheng, G., & Yu, J. (2020). A micro freeze-thaw damage model of concrete with fractal dimension. *Construction and Building Materials*, 257. https://doi.org/10.1016/j.conbuildmat.2020.119434

Lemaitre, J. (1985). A Continuous Damage Mechanics Model for Ductile Fracture. *Journal of Engineering Materials and Technology*, *107*(1), 83-89. https://doi.org/10.1115/1.3225775

Li, J., Qiao, H., & Zhu, F. (2020). Reliability analysis of fibre concrete freeze thaw damage based on the Weibull method. *Emerging Materials Research*, *9*(1), 70-77. https://doi.org/10.1115/1.3225775

Li, Q. B. (2017). *Mechanics of concrete fracture damage*. Beijing: science press.

Li, Y., Zhai, Y., Liang, W., et al. (2020). Dynamic Mechanical Properties and Visco-Elastic Damage Constitutive Model of Freeze-Thawed Concrete. *Materials*, *13*(18).

Liu, H. Y., & Su, T. M. (2016). A dynamic damage constitutive model for a rock mass with non-persistent joints under uniaxial compression. *Mechanics Research Communications*, *77*, 12-20. https://doi.org/10.1016/j.mechrescom.2016.08.006

Liu, M.-H., & Wang, Y.-F. (2012). Damage Constitutive Model of Fly Ash Concrete under Freeze-Thaw Cycles. *Journal of Ma terials in Civil Engineering*, *24*(9), 1165-1174. https://doi.org/10.1061/(ASCE)MT.1943-5533.0000491

Niu, D. T., & Xiao, Q. H. (2010). Analysis of freeze-thaw damage characteristics and life prediction of concrete. *Journal of Xi'an University of Architecture and Technology* (Natural Science Edition), *42*(3), 319-322+328.

Qiu, J., Zhou, Y., Vatin, N. I., et al. (2020). Damage constitutive model of coal gangue concrete under freeze-thaw cycles. *Construction and Building Materials*, 264. https://doi.org/10.1016/j.conbuildmat.2020.120720

Qu, G., Zheng, M., Wang, X., et al. (2023). A Freeze-Thaw Damage Evolution Equation and a Residual Strength Prediction Model for Porous Concrete Based on the Weibull Distribution Function. *Journal of Materials in Civil Engineering*, *35*(5). https://doi.org/10.1061/(ASCE)MT.1943-5533.0004745

Si, Z., Du, X., Huang, L., et al. (2020). Meso-Scale Failure of Freezing-Thawing Damage of Concrete under Uniaxial Compression. *Applied Sciences-Basel*, *10*(4). https://doi.org/10.1061/(ASCE)MT.1943-5533.0004745

Sun, M., Xin, D., & Zou, C. (2019). Damage evolution and plasticity development of concrete materials subjected to freeze-thaw during the loading process. *Mechanics of Materials*, 139. https://doi.org/10.1061/(ASCE)MT.1943-5533.0004745

Wang, B., Pan, J., Fang, R., et al. (2020). Damage model of concrete subjected to coupling chemical attacks and freeze-thaw cycles in saline soil area. *Construction and Building Materials*, 242. https://doi.org/10.1016/j.conbuildmat.2020.118205

Wang, B., Wang, F., & Wang, Q. (2018). Damage constitutive models of concrete under the coupling action of freeze-thaw cycles and load based on Lemaitre assumption. *Construction and Building Materials*, *173*, 332-341. https://doi.org/10.1016/j.conbuildmat.2018.04.054

Wang, B.-X., Pan, C., Wang, F., & Wang, Q. (2019). Concrete freeze-thaw damage evolution law based on logistic model. *Silicate Bulletin*, *38*(8), 2536-2541+2548.

Wang, J. R., Chen, Y. L., & Fu, Y. (2019). Research on fracture properties of concrete with different precast cracks under freeze-thaw environment. *Journal of Water Resources and Water Engineering*, *30*(2),178-185.

Wardeh, G., & Ghorbel, E. (2015). Prediction of fracture parameters and strain-softening behaviour of concrete: Effect of frost action. *Materials and Structures*, *48*(1-2), 123-138. https://doi.org/10.1617/s11527-013-0172-8

Xiao, Q. H., & Niu, D. T. (2009). *Cumulative Damage for Concrete in Freezing-Thawing Circumstance Based on the Weibull Distribution: Modelling and Analysis*. proceedings of the 2nd International Conference on Modelling and Simulation, Manchester, ENGLAND, F 2009 May 21-22, 2009 [C]. 2009.

Xiao, Q.-H. (2013). *Analysis of fatigue and cumulative damage characteristics for concrete in freezing-thawing environment*. Proceedings of the 11th International Conference on Fracture and Damage Mechanics, Xian, PEOPLES R CHINA, F 2013 Sep 18-21, 2012 [C]. 2013.

Yi, C., Lai, S., Zhu, H., et al. (2013). *Freeze-thawing Damage Model of New-to-old Concrete with Different Rough Interfaces; proceedings of the 2nd International Conference on Civil*. Architectural and Hydraulic Engineering (ICCAHE 2013), Zhuhai, PEOPLES R CHINA, F 2013 Jul 27-28, 2013 [C]. 2013. https://doi.org/10.4028/www.scientific.net/AMM.405-408.2707

Yu, H., Ma, H., & Yan, K. (2017). An equation for determining freeze-thaw fatigue damage in concrete and a model for predicting the service life. *Construction and Building Materials*, *137*, 104-116. https://doi.org/10.1016/j.conbuildmat.2017.01.042

Yu, J. F. (2015). *Research on the effect of cracks on the durability of concrete*. Hebei University of Technology.

Yu, X. M., & Ren, Q. W. (2010). Fracture energy test of ordinary concrete under freeze-thaw cycle. *Journal of Hohai University* (Natural Science Edition), *38*(1), 80-82.